Journal of the Geological Society, London, Vol. **153,** 1996, pp. 515–523, 7 figs. 2 tables. Printed in Northern Ireland

Early Cretaceous denudation related to convergent tectonics in the Baikal region, SE Siberia

P.A. VAN DER BEEK[1,2], D. DELVAUX[3], P.A.M. ANDRIESSEN[1] & K.G. LEVI[4]

[1]*Faculty of Earth Sciences, Vrije Universiteit Amsterdam, Netherlands*

[2]*Present address: Research School of Earth Sciences, Australian National University, Canberra ACT 0200, Australia*

[3]*Department of Geology and Mineralogy, Royal Museum for Central Africa, Tervuren, Belgium*

[4]*Institute of the Earth's Crust, Siberian Academy of Sciences, Irkutsk, Russia*

Abstract: We present 24 new apatite fission track (AFT) ages and 18 track length measurements from the Baikal region, SE Siberia. Most samples have AFT ages between 140 and 100 Ma, with relatively high mean track lengths (*c.* 13.2 μm). The relationship between AFT ages, elevation and mean track lengths indicate that the samples record rapid cooling during the Early Cretaceous (140–120 Ma), as also shown by thermal history inversion of track length distributions. Cooling took place during a Late Jurassic–Early Cretaceous orogenic phase, related to closure of the Mongol–Okhotsk ocean and reflected in the exhumation of metamorphic core complexes followed by thrusting and reverse faulting, basin inversion and large vertical motions. The variation in AFT ages throughout the study area can be partly explained by differences in geothermal structure but differential denudation also played a role. Minimum amounts of Early Cretaceous denudation are estimated at 2–3 km.

Keywords: Mesozoic, Baikal region, fission track dating, denudation.

The Baikal rift in southeastern Siberia has become one of the type examples for continental rifting. The evolution of the rift is strongly influenced by the pre-existing tectonic fabric, which developed during a protracted history of pre-rift orogenic evolution (eg., Logatchev & Zorin 1992). Therefore, an understanding of the pre-rift geodynamic evolution of the Baikal region is essential to understand the Cenozoic evolution of the rift zone.

The Baikal rift developed at the southern margin of the Siberian platform, along the suture with the Central Asian fold belt (Fig. 1). The pre-rift tectonic history of the area is linked to the opening and closure of the Palaeo-Asian and Mongol–Okhotsk oceans, during Late Proterozoic to Mesozoic times (e.g., Zonenshain *et al.* 1990). A Late Palaeozoic–Early Mesozoic phase of continental break-up, followed by Mesozoic convergence, is recognized throughout central Asia (cf. Allen *et al.* 1991; Ermikov 1994; Parfenov *et al.* 1995). The importance of Mesozoic deformation in the area has been realised for some time but the associated vertical motions have not been quantified before.

During recent years, apatite fission track thermochronology has been established as an efficient technique to study intra-plate vertical motions that were accompanied by regional denudation (e.g., Foster & Gleadow 1992; Brown *et al.* 1994; Hendrix *et al.* 1994). In this paper, we present apatite fission track data that record an important Early Cretaceous phase of cooling and denudation in the Baikal region. We interpret these data within the framework of the tectonic evolution of Central Asia and discuss the relevance towards understanding the morphotectonics of the Baikal rift zone.

Late Proterozoic–Mesozoic evolution of the Baikal region

The Baikal rift is bordered to the northwest by the Archaean–Early Proterozoic Siberian craton, which is covered by Late Proterozoic, Palaeozoic and Mesozoic platform sediments. To the southeast, the basement consists of the poly-stage Sayan–Baikal fold belt (Figs 1 & 2). The Sayan–Baikal fold belt originated from Silurian–Devonian closure of the Palaeo-Asian ocean and collision of several 'Trans-baikalian' micro-continents with the Siberian craton to the north (Berzin & Dobretsov 1994; Melnikov *et al.* 1994). A significant proportion of the belt is composed of Devonian late/post orogenic granitic plutons.

Late Palaeozoic–Early Mesozoic extension along the southern border of the Siberian craton is recorded by basin formation and magmatism (Allen *et al.* 1991; Ermikov 1994) and marks the opening of the Mongol–Okhotsk ocean. From Late Permian to Late Jurassic times the southern border of the Siberian craton developed in an active margin setting, until collision of the Siberian and Northern Chinese cratons took place in the Early Cretaceous (Zonenshain *et al.* 1990; Scotese & Golonka 1992; Enkin *et al.* 1992). To the south east of Lake Baikal, an en-echelon chain of narrow extensional basins developed during the Late Triassic, which are filled by Triassic–Jurassic volcanics and continental/limnic sediments (Fig. 2). Late Jurassic–Early Cretaceous mega-breccias and conglomerates unconformably overlie the earlier basin fill and are related to basin inversion (Ermikov 1994). The basement highs between these basins have been interpreted as metamorphic core complexes which were regarded to have developed during Late Palaeozoic

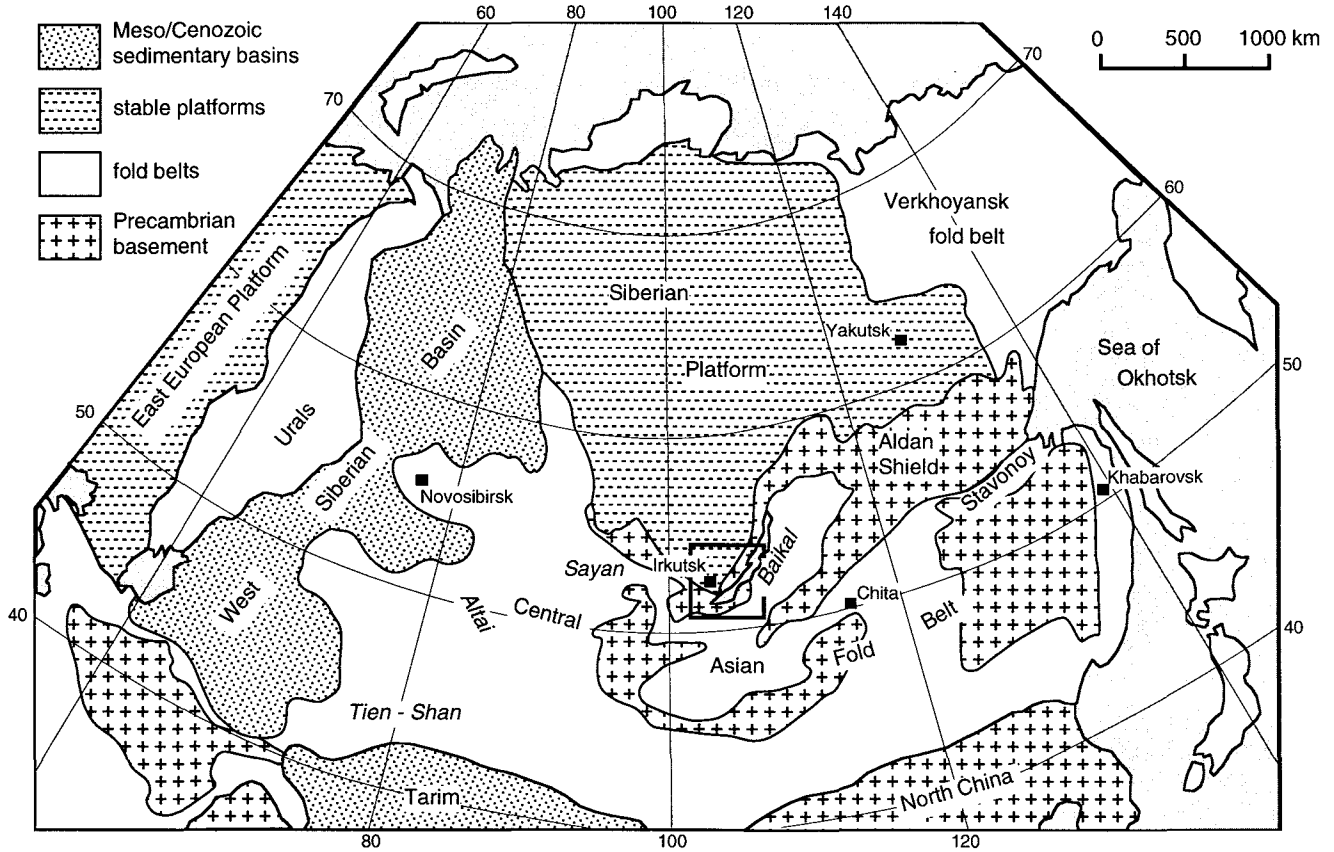

Fig. 1. Generalized tectonic map of Siberia and adjacent regions. Modified and simplified from Zonenshain *et al.* (1990). Inset shows extent of study area (Fig. 2).

extension (e.g., Melnikov *et al.* 1994). New K–Ar data, however, suggest Early Cretaceous (113–100 Ma) ages for the final exhumation of these massifs (Sklyarov *et al.* 1994).

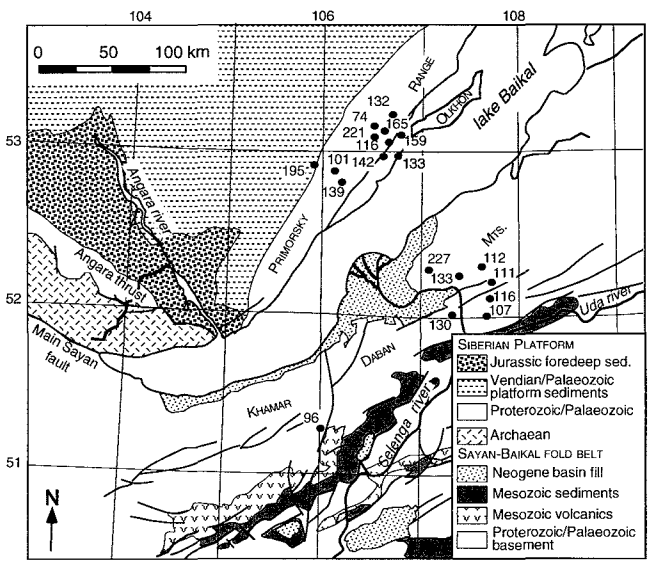

Fig. 2. Simplified tectonic map of southern and central Baikal, with emphasis on Mesozoic structures. Apatite fission track samples are indicated by their ages; to avoid clutter not all samples from the Priolkhon area have been plotted. Modified from Delvaux *et al.* (1995).

Trachy-basaltic volcanics and dykes have radiometric ages as young as 127–100 Ma (Ermikov 1994). Thus, closure of the Mongol–Okhotsk ocean seems to have been accompanied by a complex Cordilleran-type interplay of extensional and compressional phases within the Trans-Baikal fold belt. A late Early Cretaceous phase of N–S compression has, however, been clearly demonstrated from microstructural analyses in and around the inverted basins (Delvaux *et al.* 1995); its age is constrained by structural and stratigraphic relationships with the volcano-sedimentary succession. Compressional deformation affected a wide area, including the fold belt as well as the Siberian Platform (Ermikov 1994; Delvaux *et al.* 1995). To the west of Lake Baikal, Mesozoic vertical motions are recorded by the Jurassic West Baikal foredeep, which developed along the southern margin of the Siberian Platform (Fig. 2). This (foreland ?) basin was overthrust by Archaean basement along the Angara thrust during the Cretaceous.

During a period of tectonic quiescence in the Late Cretaceous–Palaeogene, the pre-existing orogen was peneplained in a warm and humid climate, causing the formation of kaolinite–laterite palaeosols (Mats 1993; Kashik & Mazilov 1994). Cenozoic rifting was underway by the mid-Oligocene (Logatchev 1993; Mats 1993). The preservation of pre-rift weathering remnants suggests that subsequent erosion was minimal (Mats 1993). The Baikal rift developed as a series of asymmetric half-graben, with the border-zone of the Siberian craton (Primorsky–Obruchevsky faults) acting as the main border fault system (Fig. 2). To the southeast, the basement gradually

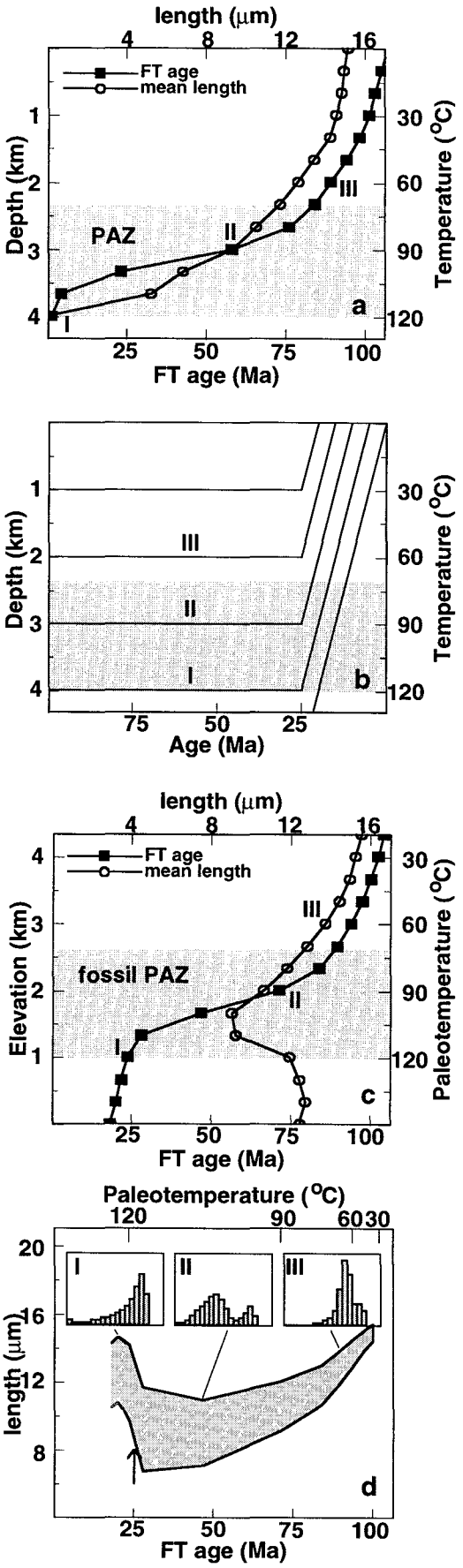

rises; the Khamar Daban range, which forms the eastern flank of the rift, is not cut by border faults. The Primorsky and Obruchevski faults enclose the Olkhon block, which can be regarded as a very large tilted fault block (Mats 1993). Two main stages are recognized within the evolution of the rift (Logatchev 1993; Mats 1993): an older (Oligocene–mid Pliocene) phase of slow rifting, low relief and low-energy sedimentation and a younger (mid-Pliocene–Recent) phase of rapid basin deepening, major relief generation and coarse clastic sedimentation.

Apatite fission track thermochronology

Over the past decade, apatite fission track (AFT) thermochronology has become a well established and widely used technique to constrain the low temperature (<120 °C) thermal histories of rocks (cf. Brown *et al.* 1994 for a review). Under tectonically stable conditions, AFT ages and mean track lengths will decrease systematically with increasing temperature (and hence depth) as a result of progressive annealing of fission tracks (Fig. 3a). The main control on the pattern of AFT ages and track lengths is exerted by the geothermal gradient; secondary controls are exerted by the duration of tectonically stable conditions and the chemical composition of the apatites (Green *et al.* 1989*a*). At temperatures between *c.* 70 and 120 °C, in the partial annealing zone (Wagner 1979), the amount of annealing increases rapidly towards total.

When a tectonic block cools as a result of exhumation, remnants of the characteristic AFT age/depth pattern may be retained, producing a trend of increasing AFT ages with elevation (Fig. 3b & c). The base of the fossil (exhumed) partial annealing zone, when exposed, will produce a characteristic break in slope in the age/elevation plot, the age of which approximates the initiation of cooling/exhumation (Gleadow & Fitzgerald 1987). Samples from below the break in slope were exhumed from temperatures ≥120 °C, and contain only tracks formed during and after cooling. In contrast, samples above the break in slope contain two generations of tracks, one from before and one from after the onset of cooling. The actual shape of the age/elevation plot, and the trend of track length distributions with elevation, will depend on the amount and rate of exhumation (Brown *et al.* 1994).

Fig. 3. (**a**) Variation of fission track age and mean track length with temperature, calculated using the annealing model of Laslett *et al.* (1987), for a 100 Ma stable thermal regime. A depth scale is added assuming a 30 °C km^{-1} geotherm. Both fission track age and mean track length decrease rapidly between *c.* 70 and 120 °C in the partial annealing zone (PAZ). (**b**) Exhumation paths of rocks from different structural levels for a history of 5 km of exhumation from 25 Ma onwards; labels I, II and III indicate rocks exhumed from below, within and above the PAZ (shaded) and are also indicated in the other plots. (**c**) Resulting pattern of fission track ages and mean track lengths, the base of the fossil PAZ is characterized by a break in slope in the age/elevation plot and records the amount of exhumation as well as the timing of its onset. (**d**) Resulting age/length plot; shaded area represents mean length ± standard deviation for samples from different palaeotemperatures (scale on top). Samples from the base of the fossil PAZ produce the low-age peak in the diagram and date the onset of exhumation. Insets show modelled fission track length distributions for 'samples' I, II and III.

The dependence of observed track length distributions (Gleadow *et al.* 1986) on thermal history can also be used to constrain the amount and timing of exhumation. A plot of fission track age against mean track length of an area that has undergone cooling will show a characteristic 'boomerang' shape (Fig. 3d); the length peak at young ages corresponds to samples which were exhumed from the base of the partial annealing zone, and thus retain only tracks formed after the onset of cooling (e.g., Omar *et al.* 1989). The kinetics of annealing in apatite are now becoming understood in a quantitative manner (Laslett *et al.* 1987; Green *et al.* 1989*b*; Lutz & Omar 1991). As a result, AFT thermochronology is presently able to record not only the amount and timing of cooling of a sample, but also to reconstruct its cooling trajectory (T–t path) below 120 °C.

It should be noted that fission track thermochronology strictly records cooling of a sample only. Where fission track data show the characteristic relationship to elevation described above, or when additional geological data are available (e.g., absence of contemporaneous magmatic or geothermal activity, correspondence of cooling intervals with periods of sediment deposition in nearby sedimentary basins, presence of planation surfaces of corresponding age), cooling can be interpreted to result from exhumation. The amount of exhumation can be quantified if the geothermal gradient is known; in most cases, cooling from 120 °C represents 3.5 ± 1 km of exhumation.

Denudation history of the Baikal region from fission track thermochronology

Sampling and procedures

Samples for fission track analysis were collected from the marginal mountains flanking both sides of the present-day rift (cf. Fig. 2). A list of sample locations and lithologies is given in Table 1. To the NW of the rift, an age/elevation profile was collected in the Primorsky range, as well as a profile across it. A number of samples were taken from the Olkhon block in the Priolkhon region. Samples from the NW of the rift comprise mainly high-grade Proterozoic basement rocks. One sample (BAI 16) was taken from the basal (Vendian) unit of the Siberian platform succession. To the SE of the rift, samples were collected in the Khamar Daban range, both north and south of the Selenga river valley. Here, all samples were Palaeozoic plutonic and metamorphic rocks. Sample preparation and processing techniques are outlined by van der Beek (1995) and follow the criteria defined by Hurford & Green (1983) and Hurford (1990).

Results

Apatite fission track (AFT) age and mean track length data are summarised in Table 2. All ages are reported as central ages (Galbraith & Laslett 1993) with $\pm 1\sigma$ errors. They show a relatively large spread, varying between 57 ± 10 and 227 ± 19 Ma. Ages significantly younger than 100 Ma were, however, only encountered in samples from the Primorsky

Table 1. *Sample details*

Sample	VUA lab. no.	Location	Latitude	Longitude	Elev. (m)	Lithology
BA058	1184	Sarminski Gonets	N53:02:44	E106:42:23	1040	Mylonitic gneiss
BA060	1182	Sarminski Gonets	N53:03:17	E106:42:00	1180	Sheared granite
BA061	1183	Sarminski Gonets	N53:03:55	E106:39:51	1330	Sheared granite
BAI 1	1154	Sarma river mouth	N53:07:44	E106:50:00	500	Mylonitic qz-fsp gneiss
BAI 2	1155	Sarma river mouth	N53:08:00	E106:50:41	720	Mylonitic qz-fsp gneiss
BAI 3	1156	Sarma river mouth	N53:08:00	E106:50:55	960	Qz–fsp–bi gneiss
BAI 4	1157	Sarma river mouth	N53:08:32	E106:50:55	1050	Felsic gneiss
BAI 5	1158	Sarma river mouth	N53:08:32	E106:50:14	820	Qz–fsp–bi gneiss
BAI 6	1159	Muchar bay	N53:01:52	E106:45:14	455	Amphibolite
BAI 7	1160	'989 peak'	N52:57:41	E106:48:52	990	Metagabbro
BAI 8	1161	'989 peak'	N52:58:56	E106:48:25	830	Gt bearing qz–fsp–bi gneiss
BAI 9	1162	'989 peak'	N52:59:36	E106:47:03	625	Amphibolite
BAI 10	1163	Olkhon gate	N53:00:48	E106:54:33	455	Qz–fsp–bi gneiss
BAI 11	1164	'989 peak'	N52:56:32	E106:47:57	455	Chl bearing quartzite
BAI 14	1165	Tyrdan quarry	N52:44:36	E106:19:15	675	Metagabbro
BAI 15	1166	Kyret river	N52:48:16	E106:15:00	730	Schistose rapakivi granite
BAI 16	1167	Kodja Stej village	N52:50:56	E106:03:58	730	Vendian sandstone
BAI 17	1168	Barguzin road	N51:56:14	E107:41:53	1020	Granite
BAI 18	1169	Barguzin road	N51:58:39	E107:42:04	1200	Bi–fsp bearing meta-arkose
BAI 19	1170	'1349 peak'	N52:01:05	E107:44:04	1300	Granite
BAI 20	1171	Irkilik valley	N52:07:00	E107:45:23	700	Diorite
BAI 21	1172	Ostrog village	N52:09:57	E107:26:37	500	Leucocratic migmatite
BAI 22	1173	road to Chergino	N52:12:23	E107:09:10	700	Metagabbro
BAI 27	1176	'1510 peak'	N51:23:02	E106:01:07	1250	Quartzite
BAI 30	1179	Sarmen Edzje mnt	N51:16:41	E106:10:19	1030	Metadacite
BAI 32	1180	Otsjurkovo quarry	N51:56:30	E107:26:42	640	Ap bearing diorite

Table 2 *Apatite fission track analytical data*

Sample	Elev. (m)	No. grains	$\rho_s N_s$ ($\times 10^6$ cm^{-2})	$\rho_i(N_i)$ ($\times 10^6$ cm^{-2})	$\rho_d(N_d)$ ($\times 10^6$ cm^{-2})	$P(\chi^2)$ (%)	Age $\pm 1\sigma$ (Ma)	D (%)	*Mean length* (μm)	*St. dev.* (μm)	*No. of tracks*
Primorsky range (W of Lake Baikal)											
BA058	1040	18	0.193 (228)	0.632 (374)	0.025(3111)	75	87 ± 9	12			
BA060	1180	13	0.654 (58)	0.327 (145)	0.025(3111)	75	57 ± 10	9			
BA061	1330								12.8 ± 0.2	1.1	36
BAI 1	500	16	0.455 (292)	0.838 (269)	2.690(3314)	25	159 ± 17	14	12.0 ± 0.2	1.2	40
BAI 2	720	20	1.035 (668)	1.791 (578)	0.025(3111)	25	165 ± 14	13	12.3 ± 0.2	1.3	65
BAI 3	960	19	0.204 (212)	0.505 (262)	2.690(3314)	$\ll 1$	132 ± 22	57			
BAI 4	1050	20	0.067 (85)	0.295 (187)	2.690(3314)	2.5	74 ± 12	30			
BAI 5	820	20	0.130 (145)	0.166 (92)	0.025(3111)	99	221 ± 32	10			
BAI14	675	20	1.018 (862)	2.189 (927)	2.690(3314)	2.5	139 ± 10	15	13.4 ± 0.1	1.0	100
BAI15	730	20	0.330 (299)	0.921 (417)	0.025(3111)	25	101 ± 10	12			
BAI16	730	20	0.823 (654)	1.258 (500)	2.690(3314)	10	195 ± 16	15	12.6 ± 0.1	1.3	102
Priolkhon area/Olkhon block (W. of Lake Baikal)											
BAI 6	455	18	1.245 (719)	3.227 (932)	2.690(3314)	50	116 ± 9	11	13.7 ± 0.1	1.0	100
BAI 7	990	15	1.877(1162)	4.248(1315)	2.690(3314)	50	132 ± 9	10	13.6 ± 0.1	1.1	102
BAI 8	830	16	1.547(1144)	3.065(1133)	0.025(3111)	10	142 ± 11	13	13.6 ± 0.1	1.1	100
BAI 9	625	17	0.670 (412)	1.634 (502)	2.690(3314)	$\ll 1$	130 ± 14	30	13.7 ± 0.1	1.1	100
BAI10	455	20	1.642(1335)	3.910(1590)	0.025(3111)	25	120 ± 9	11	13.3 ± 0.1	0.9	100
BAI11	455	19	0.970 (490)	2.110 (533)	2.690(3314)	2.5	133 ± 14	24			
Khamar Daban mountains (E of Lake Baikal)											
BAI17	1020	20	2.954(1911)	8.252(2669)	2.690(3314)	1	107 ± 6	14	13.1 ± 0.1	1.1	101
BAI18	1200	20	1.578 (858)	4.069(1106)	2.690(3314)	$\ll 1$	116 ± 9	22	13.4 ± 0.1	1.1	100
BAI19	1300	20	0.909 (739)	2.504(1018)	2.690(3314)	75	111 ± 8	9	13.3 ± 0.1	1.0	100
BAI20	700	20	2.378(1073)	6.502(1467)	2.690(3314)	75	112 ± 7	9	12.6 ± 0.1	0.9	70
BAI21	500	18	0.772 (897)	1.727(1003)	2.690(3314)	25	133 ± 9	12			
BAI22	700	20	1.155 (578)	1.526 (382)	2.690(3314)	10	227 ± 19	15	13.8 ± 0.1	1.0	100
BAI27	1250	15	0.653 (410)	0.201 (630)	0.025(3111)	50	96 ± 9	12	12.7 ± 0.2	1.3	30
BAI30	1030								13.2 ± 0.1	1.1	100
BAI32	640	14	0.173(273)	0.377(297)	0.025(3111)	99	130 ± 14	6	13.5 ± 0.2	1.2	30

Notations: ρ_s = spontaneous track density; ρ_i = induced track density (includes 0.5 geometry factor); ρ_d = density of tracks in the glass dosimeter; N_s, N_i, N_d = number of tracks actually counted to determine the reported track densities. All ages are reported as central ages (Galbraith & Laslett 1993); calculated with $\zeta = 113.6 \pm 3.8$ for glass dosimeter CN2 ($\rho_d = 2.690 \times 10^6$ cm^{-2}) and $\zeta = 11493 \pm 522$ for NBS963 ($\rho_d = 0.025 \times 10^6$ cm^{-2}). $P(\chi^2)$ = Chi-squared probability that the single grain ages represent one population; D = age dispersion. If $P(\chi^2) < 5$ and/or $D > 15$ the single grain ages represent more than one population.

fault scarp, which yielded low-quality (strongly corroded and cloudy) apatites. Most samples have AFT ages between 140 and 100 Ma, with relatively high mean track lengths (*c.* 13.2 μm) and narrow ($\sigma < 1.1$ μm) negatively skewed track length distributions (Fig. 4).

There is no systematic geographical variation of AFT ages although, with the exception of samples from the Primorsky fault scarp, ages to the SE of the rift seem somewhat younger than those to the NW (Fig. 2). A clear variation of FT ages and track lengths with elevation does not exist (Fig. 5). Samples from the Priolkhon area (Olkhon block) and the Khamar Daban mountains display nearly vertical age/elevation profiles, with track lengths around 13.0–13.5 μm. Samples from the Primorsky range (mainly the Primorsky fault scarp) show a very large scatter, the only observable trend being an unusual decrease of AFT age with elevation. Here, nearly all mean track lengths are shorter than 13 μm. On a plot of mean track lengths against AFT age, however, the data define two clearly distinguished groups (Fig. 6). Most samples fall in a trend of decreasing track lengths from 140 Ma (*c.* 13.7 μm) down to 100 Ma (*c.* 12.6 μm), with four samples defining a separate trend from 160 Ma (*c.* 12 μm) up to 230 Ma (13.8 μm).

Interpretation

The large mean track lengths, narrow track length distributions, vertical age/elevation profiles and clear grouping into two AFT age/track length groups suggest that a rapid cooling event occurred around 140–120 Ma. Samples which record ages >150 Ma would have cooled from temperatures within the apatite partial annealing zone (*c.* 70–120 °C) during this event; samples with ages <140 Ma from temperatures >120 °C (compare Figs 3 and 6). As most track length distributions are relatively long (mean track lengths only 1–1.5 μm shorter than those recorded in undisturbed volcanics; Gleadow *et al.* 1986) and narrow, it is suggested that most samples cooled rapidly, reaching temperatures <70 °C at around 120–100 Ma. Samples from the Primorsky fault scarp, some of which record ages significantly younger than 100 Ma, are considered less reliable; their cloudy and corroded appearance suggests they could have been influenced by (fault related?) fluid leaching.

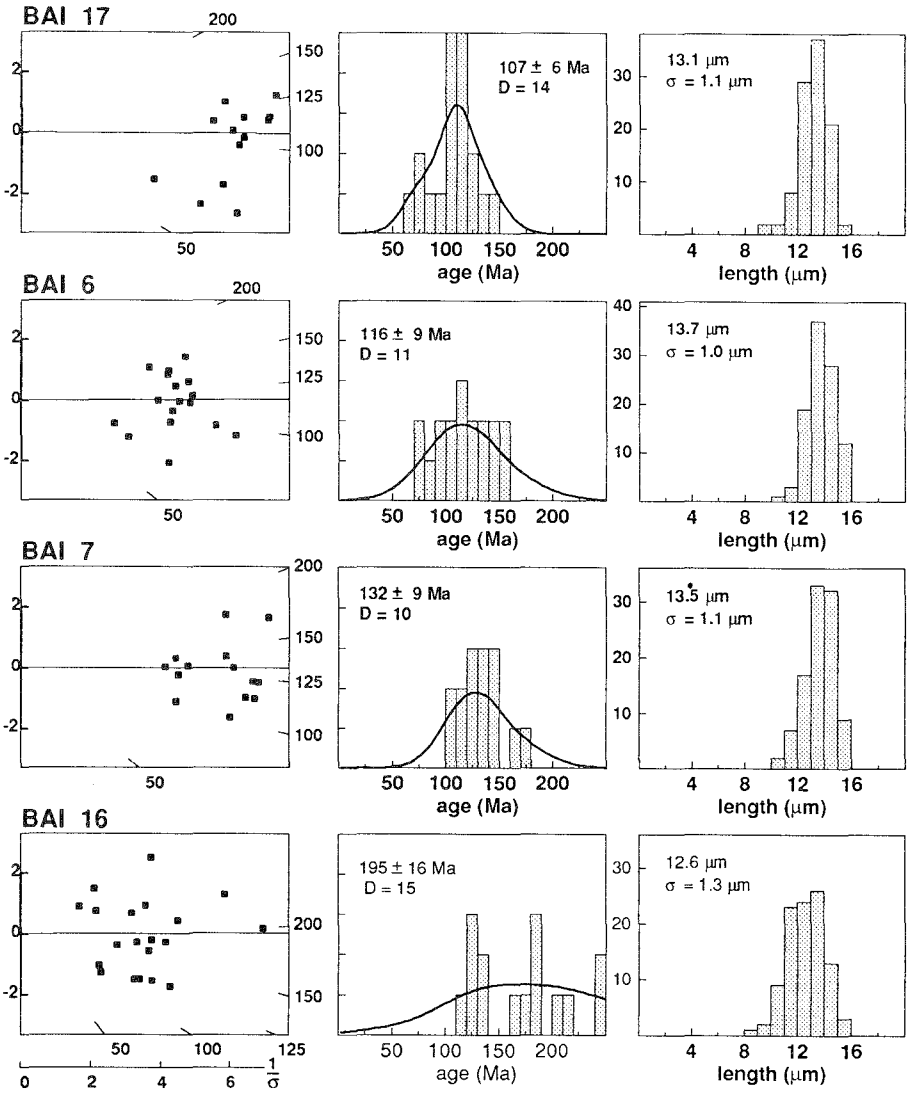

Fig. 4. Representative samples of respectively young (BAI 17), intermediate (BAI 6,7) and old (BAI 16) AFT age. Single-grain age distributions are plotted in a radial plot (left) and as age histograms and probability curves (centre). Radial plots show the precision of individual track counts on the *x*-axis and their standard error on the *y*-axis (cf. Galbraith 1990). Histograms of confined track length distributions are shown on the right.

The samples with oldest AFT ages (BAI16 and 22) record Triassic cooling (around 230–195 Ma). This first cooling phase could have brought these rocks to temperatures around 70 °C, from which they cooled during the second event. The old age and high mean track length for sample BAI22, however, also partly results from the probably high Cl-content of this sample, as indicated by very wide etch pits.

In order to asses the exhumation history of the area more quantitatively, we have inverted the track length distributions from a number of representative samples. The inversion is based on the notion that each track that is formed will experience a different portion of the thermal history of the host rock and will, therefore, exhibit a different degree of annealing (shortening). Thus, a certain thermal history can be related quantitatively to a track length distribution, using a mathematical description of the annealing process. The algorithm used (van der Beek 1995) generates random thermal histories which pass through user-defined T–t regions and calculates fission track age and length distributions from these histories. The set of thermal histories that yield ages and length distributions statistically indistinguishable from those observed define a T–t spectrum which delimits the cooling trajectory of the sample (cf. Lutz & Omar 1991).

The thermal histories obtained from inversion of track length distributions are shown in Fig. 7. We have used the annealing model of Crowley *et al.* (1991) for fluor-apatites in the inversion. Since chemical composition data for the analysed apatites are not available, we cannot justify the choice of any particular annealing model. However, the use of different models should not introduce large differences in the thermal histories obtained (cf. van der Beek 1995). The results are consistent with the qualitative interpretation of the data given above. Rapid cooling from temperatures >120 °C at around 140 Ma to *c.* 70 °C at around 120 Ma is a feature displayed by practically all samples (e.g., BAI 6,7,17). Some samples (BAI 16,17) may have remained at temperatures of around 60–70 °C for somewhat longer times, cooling down to surface temperatures only during the Late Cretaceous–Palaeogene. BAI 16 even shows a slight heating during the time span 140–120 Ma. As this sample was taken from the border of the Siberian platform sediments, this could indicate burial by overthrusting. However, the kinetics of annealing are not well constrained at temperatures <60–70 °C (Corrigan 1993; Ravenhurst *et*

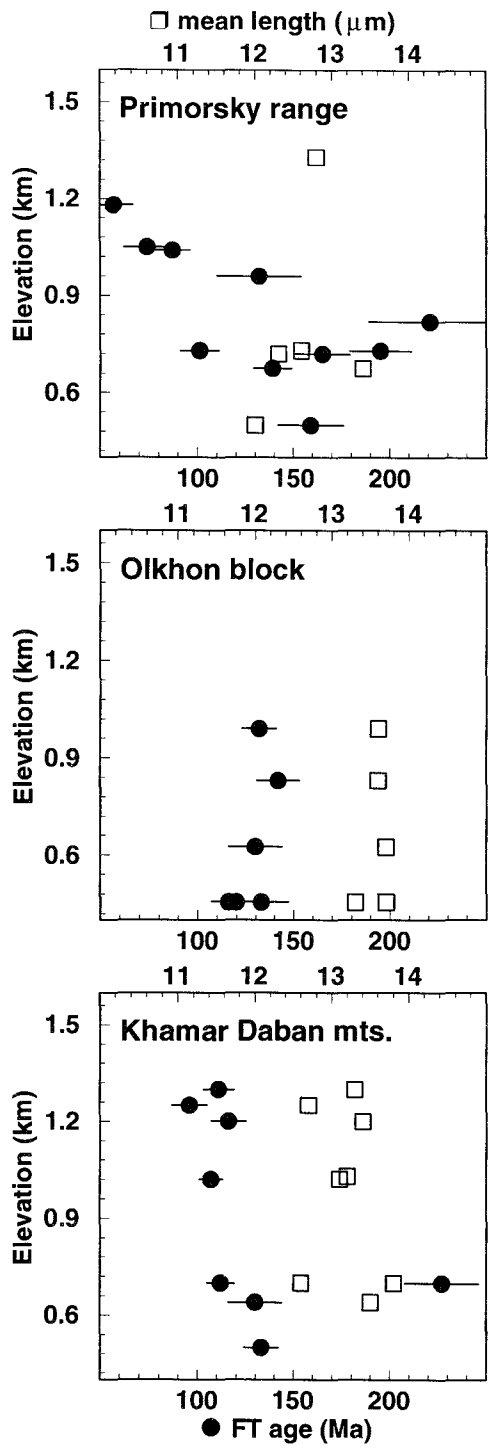

Fig. 5. Age/elevation plots for samples from the Primorsky range, the Olkhon block (both west of Lake Baikal) and the Khamar–Daban mountains (east).

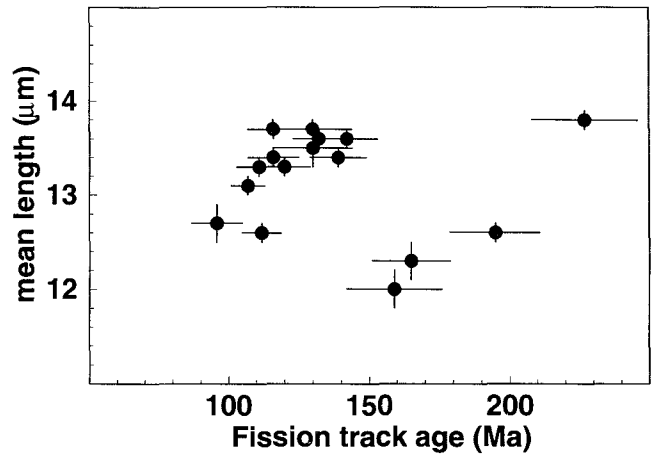

Fig. 6. Plot of mean track length against fission track age for the Baikal rift samples.

al. 1994) so that the predictions of annealing models should not be overemphasised for this temperature range.

Discussion and conclusions

The AFT data presented above suggest a rapid phase of cooling during the Early Cretaceous, contemporaneous with the final closure of the Mongol–Okhotsk ocean and collision of the Siberian and North Chinese cratons. The K–Ar data of Sklyarov *et al.* (1994) for the metamorphic core complexes to the SE of Lake Baikal also suggest final cooling in the Early Cretaceous. The area to the southeast of Lake Baikal was affected by magmatic activity during this time, as recorded by trachy-basalt flows and mafic dykes with radiometric ages of 127–100 Ma (Ermikov 1994). Jurassic coal-bearing continental deposits, occurring in the basins in this area (Fig. 2), have been affected by contact metamorphism around the dyke intrusions. Thus, the more or less random variation of AFT ages throughout the study area could be, at least partly, a result of different geothermal structure and activity throughout the area. However, differential denudation as a result of vertical block movements probably also played a role. The fact that nearly all samples record >50 °C cooling between 140–120 Ma is a

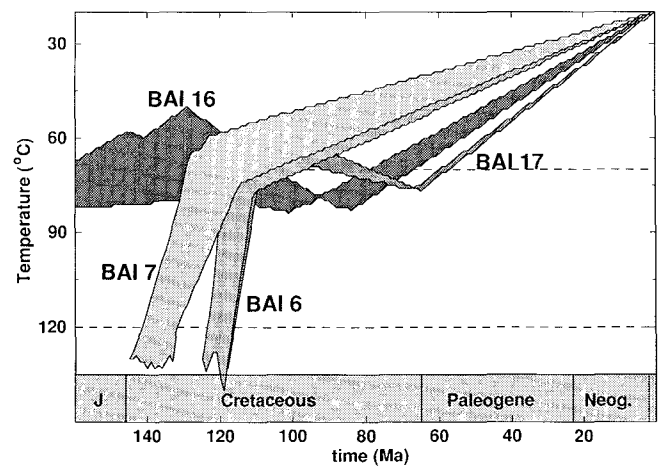

Fig. 7. Model thermal histories obtained from inverting the observed horizontal confined track length distributions (cf. van der Beek 1995) using the annealing model of Crowley *et al.* (1991) for fluor-apatites. Thermal histories within the shaded bands fit the observed AFT ages within 1σ error and pass the Kolmogorov–Smirnov test for track length distributions at the 95% confidence level (cf. Lutz & Omar 1991). Dashed lines at 70 and 120 °C delimit partial annealing zone and serve as a guide to the eye.

strong indication for regional denudation during this time. The amount of denudation is difficult to estimate because geothermal gradients for the Mesozoic are unknown, and were probably variable. However, the age/length plot (Fig. 6) suggests that samples with ages around 100 Ma and track lengths $<13\,\mu m$ (e.g., BAI17, BAI27) cooled from temperatures significantly above 120 °C (possibly around 150 °C). Even when taking very high values for the geothermal gradient (40–50 °C km^{-1}) into account, this leads to a minimum denudation estimate of 2–3 km. As a comparison, Parfenov *et al.* (1995) estimate syn-orogenic erosion in the Verkhoyansk fold belt, which was overthrust onto the NE border of the Siberian craton during the Early Cretaceous, to amount to 1.5–2.1 km from vitrinite reflectance studies.

Mesozoic denudation of the Baikal region is also documented by the widespread occurrence of a planation surface with remains of a palaeosol. The age of this planation surface is generally described as Late Cretaceous–Palaeocene, and its origin as resulting from post-orogenic peneplanation (e.g., Mats 1993; Kashik & Mazilov 1994). The fission track data presented here suggest that the onset of exhumation took place already during the Early Cretaceous, i.e. syn-orogenic. The elevation of the Cretaceous-Palaeogene planation surface, which is widely encountered around Lake Baikal, has been used as a pre-rift reference surface (Logatchev 1993; Mats 1993). The AFT data indicate that very little erosional denudation has affected the flanks adjacent to the central Baikal rift since the onset of rifting.

Fieldwork in the Baikal region was conducted within the framework of the CASIMIR project, co-ordinated by J. Klerkx (Royal Museum for Central Africa, Tervuren) and N.A. Logatchev (Institute of the Earth's Crust, Irkutsk, Russia). Support in the field was provided by S. Kuzmin, V. Sankov, R. Moeys and G. Stapel. L. IJlst and T. Vogel-Eissens assisted in sample preparation and processing. Irradiations were carried out at the Dutch Energy Research Centre (ECN) in Petten. We thank B. Windley, M. Zentilli and an anonymous Geological Society internal reader for constructive reviews. Netherlands Research School of Sedimentary Geology Publication no. 960103. Correspondence to P. A. van der Beek (e-mail: peter@rses.anu.edu.au)

References

ALLEN, M.B., WINDLEY, B.F., ZHANG, C., ZHAO, Z.-Y. & WANG, G.-R. 1991. Basin evolution within and adjacent to the Tien Shan Range, NW China. *Journal of the Geological Society, London*, **148,** 369–378.

BERZIN, N.A. & DOBRETSOV, N.I. 1994. Geodynamic evolution of Southern Siberia in Late Precambrian—Early Palaeozoic time. *In*: COLEMAN, R.G. (ed.) *Reconstruction of the Paleo-Asian Ocean*. VSP International Science Publishers, the Netherlands, 45–62.

BROWN, R.W., SUMMERFIELD, M.A. & GLEADOW, A.J.W. 1994. Apatite fission-track analysis: Its potential for the estimation of denudation rates and implications for models of long-term landscape development. *In*: KIRKBY, M.J. (ed.) *Process Models and Theoretical Geomorphology*. Wiley, New York, 24–53.

CORRIGAN, J. 1993. Apatite fission-track analysis of Oligocene strata in South Texas, U.S.A.: Testing annealing models. *Chemical Geology (Isotope Geoscience Section)*, **104,** 227–249.

CROWLEY, K.D., CAMERON, M. & SCHAEFER, R.L. 1991. Experimental studies of annealing of etched fission tracks in fluorapatite. *Geochimica et Cosmochimica Acta*, **55,** 1449–1465.

DELVAUX, D., MOEYS, R., STAPEL, G., MELNIKOV, A. & ERMIKOV, V. 1995. Paleostress reconstructions and geodynamics of the Baikal region, Central Asia. Part I: Paleozoic and Mesozoic pre-rift evolution. *Tectonophysics*, **252,** in press.

ENKIN, R.J., YANG, Z., CHEN, Y. & COURTILLOT, V. 1992. Paleomagnetic contraints on the geodynamic history of the major blocks of China from the Permian to the Present. *Journal of Geophysical Research*, **97,** 13953–13989.

ERMIKOV, V.D. 1994. Mesozoic precursors of rift structures in Central Asia. *Bulletin du Centre de Recherches d'Exploration—Production Elf Aquitaine*, **18,** 123–134.

FOSTER, D.A. & GLEADOW, A.J.W. 1992. The morphotectonic evolution of rift-margin mountains in central Kenya: Constraints from apatite fission-track thermochronology. *Earth and Planetary Science Letters*, **113,** 157–171.

GALBRAITH, R.F. 1990. The radial plot: Graphical assessment of spread in ages. *Nuclear Tracks and Radiation Measurements*, **17,** 207–214

—— & LASLETT, G.M. 1993. Statistical models for mixed fission track ages. *Nuclear Tracks and Radiation Measurements*, **21,** 459–470.

GLEADOW, A.J.W. & FITZGERALD, P.G. 1987. Uplift history and structure of the Transantarctic Mountains: new evidence from fission track dating of basement apatites in the Dry Valleys area, southern Victoria Land. *Earth and Planetary Science Letters*, **82,** 1–14.

——, DUDDY, I.R., GREEN, P.F. & LOVERING, J.F. 1986. Confined fission track lengths in apatite: a diagnostic tool for thermal history analysis. *Contributions to Mineralogy and Petrology*, **94,** 405–415.

GREEN, P.F., DUDDY, I.R., GLEADOW, A.J.W. & LOVERING, J.F. 1989*a*. Apatite fission-track analysis as a paleotemperature indicator for hydrocarbon exploration. *In*: NAESER, N.D. & MCCULLOH, T.H. (eds) *Thermal history of sedimentary basins*. Springer-Verlag, New York, 181–195.

——, ——, LASLETT, G.M., HEGARTY, K.A., GLEADOW, A.J.W. & LOVERING, J.F. 1989*b*. Thermal annealing of fission tracks in apatite 4. Quantitative modelling techniques and extension to geological timescales. *Chemical Geology (Isotope Geoscience Section)*, **79,** 155–182.

HENDRIX, M.S., DUMITRU, T.A. & GRAHAM, S.A. 1994. Late Oligocene–early Miocene unroofing in the Chinese Tien Shan: An early effect of the India–Asia collision. *Geology*, **22,** 487–490.

HURFORD, A.J. 1990. International union of geological sciences subcommission on geochronology recommendation for the standardization of fission track dating calibration and data reporting. *Nuclear Tracks and Radiation Measurements*, **17,** 233–236.

—— & GREEN, P.F. 1983. The zeta age calibration of fission-track dating. *Chemical Geology (Isotope Geoscience Section)*, **1,** 285–317.

KASHIK, S.A. & MAZILOV, V.N. 1994. Main stages and palaeogeography of Cenozoic sedimentation in the Baikal rift system (eastern Siberia). *Bulletin du Centre de Recherches d'Exploration–Production Elf Aquitaine*, **18,** 453–462.

LASLETT, G.M., GREEN, P.F., DUDDY, I.R. & GLEADOW, A.J.W. 1987. Thermal annealing of fission tracks in apatite 2. A quantitative analysis. *Chemical Geology (Isotope Geoscience Section)*, **65,** 1–13.

LOGATCHEV, N.A. 1993. History and geodynamics of the Baikal Rift (East Siberia): A review. *Bulletin du Centre de Recherches d'Exploration–Production Elf Aquitaine*, **17,** 353–370.

—— & ZORIN, YU. A. 1992. Baikal rift zone: structure and geodynamics. *Tectonophysics*, **208,** 273–286.

LUTZ, T.M. & OMAR, G.I. 1991. An inverse method of modeling thermal histories from apatite fission track data. *Earth and Planetary Science Letters*, **104,** 181–195.

MATS, V.D. 1993. The structure and development of the Baikal rift depression. *Earth Science Reviews*, **34,** 81–118.

MELNIKOV, A.I., MAZUBAKOV, A.M., SKLYAROV, E.V. & VASILJEV, E.P. 1994. Baikal rift basement: structure and tectonic evolution. *Bulletin du Centre de Recherches d'Exploration–Production Elf Aquitaine*, **18,** 99–122.

OMAR, G.I., STECKLER, M.S., BUCK, W.R. & KOHN, B.P. 1989. Fission-track analysis of basement apatites at the western margin of the Gulf of Suez rift, Egypt: evidence for synchroneity of uplift and subsidence. *Earth and Planetary Science Letters*, **94,** 316–328.

PARFENOV, L.M., PROKOPIEV, A.V. & GAIDUK, V.V. 1995. Cretaceous frontal thrusts of the Verkhoyansk fold belt, eastern Siberia. *Tectonics*, **14,** 342–358.

RAVENHUST, C.E., WILLETT, S.D., DONELICK, R.A. & BEAUMONT, C. 1994. Apatite fission track thermochronometry from central Alberta: Implications for the thermal history of the Western Canada Sedimentary Basin. *Journal of Geophysical Research*, **99,** 20023–20041.

SCOTESE, C.R. & GOLONKA, J. 1992. *PALEOMAP Paleogeographic Atlas*. PALEOMAP progress report **20,** Dept. of Geology, University of Texas at Arlington.

SKLYAROV, E.V., BELICHENKO, V.G., MAZUBAKOV, A.M., MELNIKOV, A.I. & DONSKAYA, T.V. 1994. Evolution of the Mongol–Okhotsk ocean and formation of metamorphic core complexes. *In*: *From Paleoasian Ocean to Paleo-Pacific Ocean*. Proceedings of an International joint Symposium of IGCP Projects 283, 321, 359, Sapporo, 72–74.

VAN DER BEEK, P.A. 1995. *Tectonic Evolution of Continental Rifts—Inferences*

from numerical modelling and fission track thermochronology. PhD Thesis, Vrije Universiteit Amsterdam.

WAGNER, G.A. 1979. Correction and interpretation of fission track ages. *In*: JÄGER, E. & HUNZIKER, J.C. (eds) *Lectures in Isotope Geology*. Springer Verlag, Berlin, 170–177.

ZONENSHAIN, L.P., KUZMIN, M.I. & NATAPOV, L.M. 1990. *Geology of the USSR: A Plate-Tectonic Synthesis*. American Geophysical Union Geodynamics Series, **21**.

Received 18 September 1995; revised typescript accepted 8 February 1996.
Scientific editing by Jane Evans.